INSTITUTE OF PHYSICS PUBLISHING JOURNAL OF OPTICS B: QUANTUM AND SEMICLASSICAL OPTICS

J. Opt. B: Quantum Semiclass. Opt. **4** (2002) 75–79 PII: S1464-4266(02)30947-9

Coherent exchange of momentum between atoms and light

M Cashen[1], O Rivoire[2], L Yatsenko[3] and H Metcalf[1]

[1] Physics and Astronomy, State University of New York, Stony Brook, NY 11794-3800, USA
[2] École Normale Supérieure, 45 rue d'Ulm, 75230 Paris cedex 05, France
[3] Institute of Physics, Academy of Sciences, Prosp. Nauky 46, Kiev, Ukraine

Received 19 November 2001, in final form 4 January 2002
Published 17 January 2002
Online at stacks.iop.org/JOptB/4/75

Abstract
We have demonstrated that coherent control of the momentum exchange between a light field and atoms can be implemented in frequency-modulated light. The optical parameters are chosen to drive the atoms between ground and excited states by adiabatic rapid passage in counterpropagating modulated light beams. We apply the optical force transversely to a thermal atomic beam, and the deflection provides a measure of the force. The modulation period is $2\pi/\omega_s \ll \tau$, and each half-cycle exchanges momentum $2\hbar k$, so the resulting force is much greater than the ordinary radiative force. Moreover, the velocity range of the force in such a light field is much greater than that of the radiative force. This constitutes another example of the huge range of capabilities of optical forces in non-monochromatic light.

Keywords: Laser cooling, optical forces, polychromatic light, strong optical forces, adiabatic rapid passage

1. Introduction

In ordinary Doppler laser cooling of two-level atoms, the radiative force produces both the slowing force and the dissipation necessary for cooling. The momentum exchange proceeds by absorption followed by spontaneous emission, and so there is minimal control of its nature. This radiative force saturates at a maximum value of $F_{\rm rad} \equiv \hbar k\gamma/2$, where $\lambda \equiv 2\pi/k$ is the wavelength of the optical transition, and $\gamma \equiv 1/\tau$ is the excited state decay rate. Moreover, the velocity range is confined to approximately $\pm v_c$, where $v_c \equiv \gamma/k$.

By contrast, in sub-Doppler cooling of multilevel atoms, it is typically the dipole force that works on the atoms. In this case, excited atoms return to their ground states more frequently by stimulated than spontaneous emission. The dipole force does not saturate because the de-excitation rate, and hence the momentum exchange rate, is not limited by γ. Of course, such a controllable exchange is reversible and therefore conservative, so it cannot be used for cooling: only the optical pumping among the multiple levels, enabled by spontaneous emission, can reduce the atomic phase space volume [1]. This also limits the velocity-dependent part of such forces as Sisyphus cooling in a polarization gradient to $F(v) \leqslant F_{\rm rad}$, and the velocity range to even less than $\pm v_c$.

The non-saturable dipole force seems very attractive as a tool for manipulating atoms, but its practical utility is extremely limited in an optical standing wave because its sign alternates in space on the wavelength scale so its spatial average vanishes. Only optical pumping among different sublevels mediated by spontaneous emission [2] (or different dressed state manifolds in the two-level atom case [3]) allows its extension into larger spatial domains. The desire to extend the spatial range of the dipole force has produced two independent proposals that used two frequencies to provide spatial rectification [4, 5] and these ideas were subsequently demonstrated [6–9].

The exploitation of bichromatic light for optical forces on atoms was extended by using an optical field of two beams of equal intensities and detunings that provided both a force much stronger than $F_{\rm rad}$ and a velocity range much wider than $\pm v_c$ [10]. Since the bichromatic force covers a large range of velocities, Doppler compensation is unnecessary for slowing a thermal beam. Moreover, it has a strong velocity dependence at its range boundaries so that it can cool. Naturally this (dissipative) velocity dependence originates from the occasional spontaneous emission events at a rate determined by γ, but the magnitude of the bichromatic force is not limited by this rate [10]. More recently, this form of the bichromatic force has been studied in considerable detail [11, 12], and especially

in He [13, 14]. Other schemes involving two-frequency fields have also been investigated [15].

The π-pulse model for describing the bichromatic force in light of frequencies $\omega \pm \delta$, $(\delta \gg \gamma)$ provides an intuitive description [4, 10]. With two counterpropagating beams of light, each composed of two frequencies and appropriately chosen equal amplitudes, atoms are subject to π-pulses from the beat frequency alternately from one direction and then from the other. This sequence flips the atoms from ground state to excited state and *vice versa*. In so doing, it produces a net momentum transfer of $2\hbar k$ in a time π/δ. In the absence of spontaneous emission, the force is thus $\sim 2\hbar k\delta/\pi \gg F_{\rm rad}$, and is *not* subject to saturation. Spontaneous emission reduces this by about a factor of 2 [10, 11]. Moreover, the velocity range of the bichromatic force is $\sim \pm\,\delta/2k \gg \pm v_c$.

2. The adiabatic rapid passage force

The bichromatic force is modelled in terms of π-pulses that exchange coherently the ground and excited state populations of two-level atoms. This process also mediates controlled momentum exchange without saturation. However, π-pulses are not the only way to accomplish this inversion: another way uses the well known frequency sweep technique called adiabatic rapid passage (ARP) to do it with nearly 100% efficiency [16–18].

ARP is particularly well described using an artificial 'Bloch vector' $\vec{R}$ whose components are determined by the complex coefficients of the superposition of atomic ground and excited states caused by interaction between a two-level atom and the laser light [19]. The Schrödinger equation is equivalent to a form where the time dependence of these coefficients satisfies $\mathrm{d}\vec{R}/\mathrm{d}t = \vec{\Omega}' \times \vec{R}$, where $\vec{\Omega}'$ is a 'torque' vector whose two horizontal components are the real and imaginary parts of the atomic Rabi frequency Ω in the laser field, and the vertical component is the detuning from atomic resonance δ. Thus $|\vec{\Omega}'| = \sqrt{|\Omega|^2 + \delta^2}$. (Usually Ω can be chosen to be real.)

This geometric view of the Schrödinger equation allows a particularly graphic interpretation of ARP (see figure 1). At the beginning of the frequency sweep, where the initial detuning δ_0 is much larger than the Rabi frequency Ω, $\vec{R}$ executes small, rapid orbits near the south pole (atom in the ground state), and the axis of these orbits slowly drifts up toward the equator as δ approaches zero. The sweep continues toward the opposite detuning so that near the end of the sweep, where again $\delta \gg \Omega$, $\vec{R}$ executes small, rapid orbits near the north pole, and is finally left at the north pole (the atom is in the excited state).

There are certain requirements for this process to occur efficiently. First, Ω must be large enough so that $\vec{R}$ makes very many precessions about $\vec{\Omega}'$ during the sweep time $T_{\rm s} \equiv \pi/\omega_{\rm s}$, which means $\Omega \gg \omega_{\rm s}$. This 'adiabatic following' of $\vec{\Omega}'$ by $\vec{R}$ produces the 'A' in ARP. For a uniform sweep rate, $\dot{\delta} = \delta_0\omega_{\rm s}/\pi$, where $\pm\delta_0$ is the sweep range. This means $\dot{\delta} \ll 2\delta_0\Omega$.

Second, the entire sweep must occur in a shorter time compared with the atomic excited state lifetime to minimize the effects of spontaneous emission during the sweep, and thereby preserve coherence between the atom and the radiation field. This requires $\omega_{\rm s} \gg \gamma$, or $\dot{\delta} \gg 2\delta_0\gamma$, and constitutes the 'rapid' condition in the name ARP. These are two conditions on the sweep time $T_{\rm s}$ and the Rabi frequency Ω that must be met independently, in addition to their combination $\Omega \gg \gamma$.

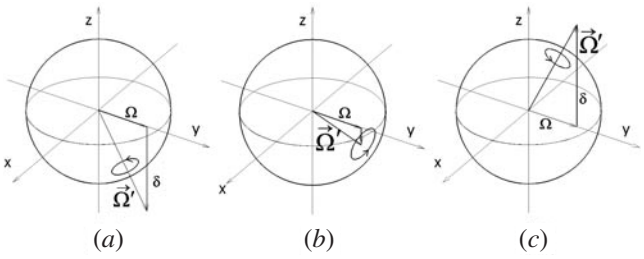

Figure 1. At the beginning of the frequency sweep with the atoms in the ground state (south pole), the initial detuning δ_0 is much larger than the Rabi frequency Ω. Thus $\vec{R}$ executes small, rapid orbits near the south pole because the 'torque' vector $\vec{\Omega}'$ is nearly polar as shown in part (*a*). These oscillations grow as δ sweeps toward 0 where the precession axis approaches the equatorial plane as shown in part (*b*). At $\delta = 0$, $\vec{R}$ executes orbits in a vertical plane because the only remaining component of the 'torque' vector $\vec{\Omega}'$ is Ω, and thus $\vec{\Omega}'$ is in the equatorial plane. Near the end of the sweep δ is again very large, $\vec{R}$ executes small, rapid orbits near the north pole as shown in part (*c*), and is finally left at the north pole with the atom in the excited state. Atoms that start at the north pole (excited state) are similarly driven in this coherent way to the south pole.

Finally, it is required that $\delta_0 \gg \Omega$ so that $\vec{\Omega}'$ is nearly polar at the extremes of the sweep. Thus δ_0 is the highest frequency in the system. All these conditions can be written together as

$$\delta_0 \gg \Omega \gg \omega_{\rm s} \gg \gamma. \tag{1}$$

ARP is a far more robust method than π-pulses for inverting the population of a two-level system. It is not sensitive to variations of the interaction time or the intensity as is the π-pulse method. Changes in the start and end point of the sweep are easily tolerated with little consequence as long as equation (1) is satisfied. Thus it seems very attractive to implement this method as a tool for coherently controlled exchange of momentum between atoms and a light field.

A simple model calculation of the magnitude of the ARP-mediated force begins by considering that the momentum transfer in one half-cycle of the frequency-modulated light is $2\hbar k$. First, a frequency-swept laser beam from one direction excites the atoms and transfers $\hbar k$, and then another beam from the opposite direction, and whose sweep is delayed, drives them back to the ground state and also transfers $\hbar k$. The direction of the frequency sweep, namely the sign of $\dot{\delta}$, is of no consequence as long as $\vec{\Omega}'$ is essentially polar at the ends of the sweep. Since the time for this is $\pi/\omega_{\rm s}$, the force is $F_{\rm ARP} \sim 2\hbar k/(\pi/\omega_{\rm s}) = 2\hbar k\omega_{\rm s}/\pi$.

As in the case of the bichromatic force, spontaneous emission compromises the strength of this force by about a factor of 2, while at at the same time enabling its dissipative character and unidirectionality [11, 12]. Thus we might expect $F_{\rm ARP} \sim \hbar k\omega_{\rm s}/\pi \gg F_{\rm rad}$. For modulation frequency $\omega_{\rm s} = 10\gamma$, this picture predicts $F_{\rm ARP} \sim 6.4F_{\rm rad}$. Of course, the model is not completely correct because the cycles of frequency-swept light overlap one another rather than being completely separated in time. Nevertheless, we have modified an existing numerical simulation program for the bichromatic force[4] to make it applicable to $F_{\rm ARP}$ and have found good

[4] This code was kindly provided to us by the authors of [10].

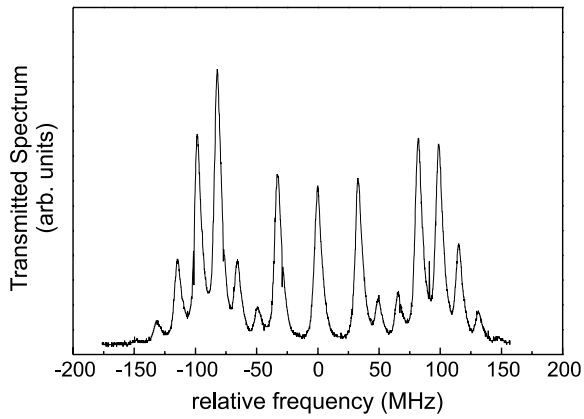

Figure 2. The laser spectrum measured with a scanning Fabry–Perot interferometer whose free spectral range is ∼1 GHz and finesse ∼200 so that it shows the sidebands well. The slight asymmetry of corresponding sideband intensities about the centre is attributed to a variation of the laser power as the injection current is varied at the rf frequency. Here $\omega_s = 10\gamma = 2\pi \times 16$ MHz and $\beta = 7$. The sidebands are clearly spaced at 16 MHz, but note the absence of the first order.

agreement between this model calculation and such numerical calculations. Moreover, the measurements described below further corroborate this model.

3. Apparatus

Our apparatus for the study of polychromatic forces on metastable He (He*) has already been described [14, 15], but is briefly reviewed here. We drive the $2^3S_1 \rightarrow 2^3P_2$ transition at $\lambda = 1083$ nm. We implemented this ARP force using amplified light from a diode-pumped fibre amplifier[5] that originates from an injection-current-modulated SDL-6702-H1 diode laser.

The free-running diode laser was frequency modulated by using a bias tee to inject an rf modulation current on top of the dc current that drives the laser diode. The modulation frequency was $\omega_s = 10\gamma = 2\pi \times 16.3$ MHz. Note that the familiar steady-state spectrum of frequency-modulated light is indeed a carrier with sidebands as shown in figure 2, but that the instantaneous frequency is swept by the rf field of frequency ω_s exactly as required for ARP. The optical electric field is $\vec{\mathcal{E}} = \vec{\mathcal{E}}_0 \cos[\omega_\ell t + \beta \sin(\omega_s t)]$ where ω_ℓ is the laser frequency and $\beta \equiv \delta_0/\omega_s$. Then the instantaneous frequency is the time derivative of the phase of $\vec{\mathcal{E}}$, namely $\omega_\ell + \delta_0 \cos(\omega_s t)$, which is just the desired frequency sweep of $2\delta_0$ in time π/ω_s.

The output beam of the diode laser was injected into a diode-pumped fibre amplifier to produce the necessary several hundred mW of frequency-modulated light[5]. The output beam of the fibre amplifier was subsequently circularly polarized to pump atoms into the $M_J = 1$ sublevel of the 2^3S_1 state and to drive the closed transition to the 2^3P_2, $M_J = 2$ sublevel. The peak intensity in each of our elliptical Gaussian laser beams (waists ∼7.5 and 1.3 mm) was ∼1.2 W cm^{-2}, about $7500 \times I_{sat}$, where the saturation intensity $I_{sat} \equiv \pi hc/3\lambda^3\tau \approx 0.16$ mW cm^{-2}. Therefore, the peak Rabi frequency $\bar{\Omega}_R$ was $\sim 60\gamma$. The diode laser alone does not produce enough power to generate this peak intensity in an adequately sized laser

[5] Made by Keopsys, Lannion, France.

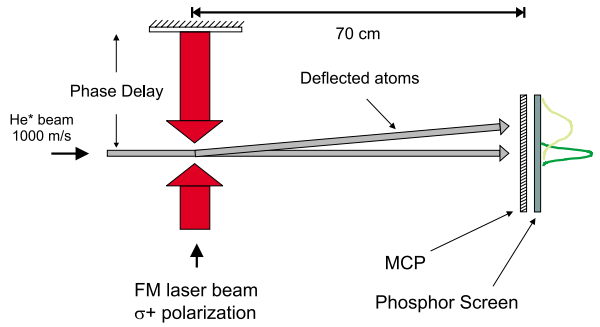

Figure 3. A top view showing the horizontal atomic beam subject to the transverse laser beams as it enters the interaction region. The plot at the end is a trace of the atomic flux across the middle of the image. Atoms are deflected by the ARP force, and their velocity distribution is broadened by the width of the longitudinal velocity distribution and by different numbers of spontaneous emission events.

(This figure is in colour only in the electronic version)

beam, but the technology of fibre amplifiers injected with diode laser light has set the stage for this whole range of new experiments.

Our atomic beam source is modelled after the reverse flow design of Kawanaka *et al* [20] with modifications originated by Mastwijk *et al* [21]. It consists of a 1 cm diameter quartz tube with a 1 mm diameter tungsten needle along its axis and a 3 cm diameter LN_2-cooled stainless steel coaxial jacket. The plasma from a dc discharge produces about $\sim 10^{14}$ He* atoms s^{-1} with a velocity distribution typical of ∼150 K. We have characterized this velocity distribution using a time-of-flight method with a tuning-fork beam chopper, and found the mean longitudinal atomic velocity to be ≈1000 m s^{-1}. The atoms passed through a vertical slit to define and collimate the beam and thereby enable one-dimensional transverse measurements of atomic deflection and/or laser cooling.

We used a microchannel plate (MCP) and phosphor screen combination to detect the He* atoms 70 cm away from the interaction region, as shown in figure 3, and we inferred their transverse velocity distribution from their spatial distribution. Since He* atoms carry about 20 eV of internal energy, they ejected an electron from the upstream surface of the MCP with high probability, and the amplified pulses at the output side of the MCP were accelerated to the screen. The screen was viewed through a window by a video camera connected to a PC via a frame grabber card. To characterize the apparatus we did several ordinary Doppler deflection experiments with a single laser beam using a wide range of laser parameters, and compared the measurements with straightforward calculations [1]. The agreement was excellent in every detail with a single laser beam to deflect the atoms, we varied the intensity, polarization and detuning of the light. We measured the deflection of the atoms, extracted the force and compared the result with the calculations. The agreement also confirmed the limits of the Doppler force in both its velocity range and magnitude. We also did single frequency laser cooling with standing waves, both with and without polarization gradients. Again, both the Doppler and the sub-Doppler cooling limits we observed were consistent with straightforward calculations.

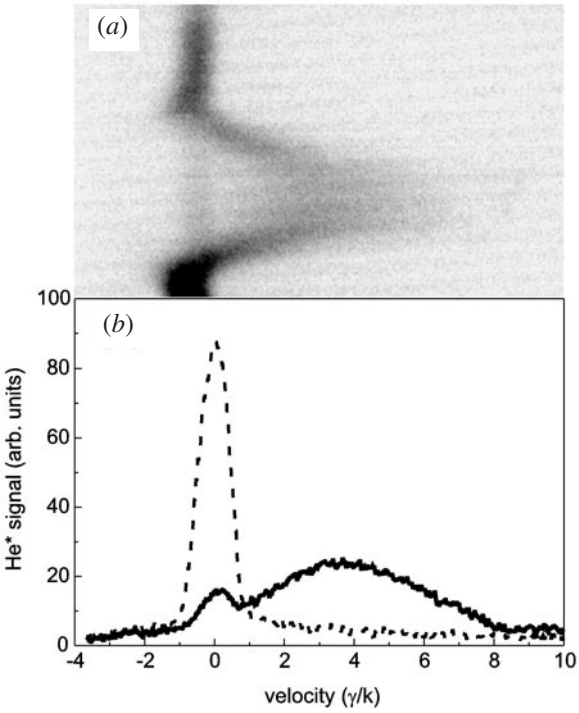

Figure 4. Part (*a*) is a single-frame image (no averaging—1/30 s frame) of the phosphor screen illuminated by electrons amplified by the MCP that are emitted by impact of He* atoms (with laser light on). The interaction time was ∼40 τ. Atoms hitting near the top and bottom of the screen do not pass through the laser beam and therefore serve as markers for undeflected atoms. The prominent bulge to the right shows the strongly deflected atoms. Part (*b*) shows a plot of the atomic flux along a line across the middle of part (*a*). The dashed line shows the unperturbed atomic distribution and the solid curve shows the positions of the deflected atoms. The peak Rabi frequency $\bar{\Omega}$ was 60γ, $\omega_s = 10\gamma$, $\phi = \pi/4$, $\beta = 10$, $\delta_0 = 100\gamma$ and centre detuning = 0.

The frequency-modulated light beam passed through an adjustable vertical slit of width d mm to limit the interaction time to $d/v \sim d\ \mu$s ∼$10\tau d$. It crossed the atomic beam, and the small absorbed fraction imparted a transverse momentum impulse $\hbar k$ to atoms in the beam during the frequency sweep that was much shorter than the passage time of the atoms through the transverse light beam. Then it travelled to a retro-reflecting mirror 120 cm away to produce the desired relative phase $\phi = \pi/4$ of the two counter-propagating frequency-swept beams. Thus the frequency-swept light returned the excited atoms to their ground states and imparted the second impulse of $\hbar k$ as described in the ARP-mediated force picture.

4. Results

As shown in figure 3 we viewed the atomic distribution at the end of the beam line with a video camera and saved the image. A typical picture is shown in figure 4(*a*), and a plot of the atomic intensity profile is shown in figure 4(*b*). From figure 4(*b*) we can determine that the average transverse velocity change of atoms deflected by this force $\Delta v \sim 3.8\gamma/k \sim 76\hbar k/M =$ 76× the recoil velocity. For an interaction time of 40τ resulting from $d = 4$ mm, this corresponds to a force of 3.8 $F_{\rm rad}$, about 3/5 of the prediction of the model. Moreover, it may be much stronger at lower velocities than at $v \sim 3.8\gamma/k$, but

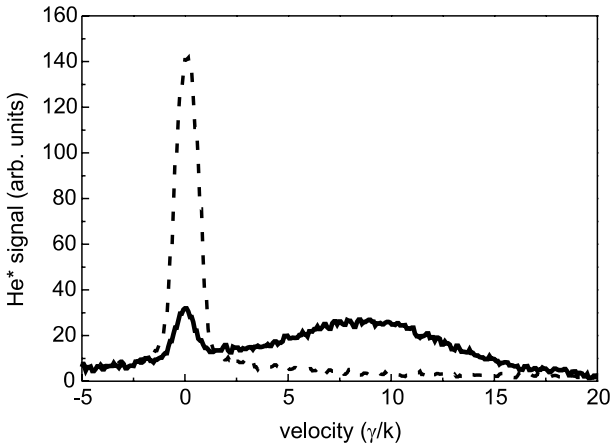

Figure 5. Similar to part (*b*) of figure 4, but in this case the modulation is not centred about atomic resonance, but 60γ above it, and the interaction time was 70τ. The dashed curve shows the unperturbed atomic distribution and the solid curve shows the positions of the deflected atoms. Here the laser parameters were the same as in figure 4 except $\phi = \pi/10$, $\beta = 7$ and centre detuning $= +60\gamma$.

our measurement is only an average over this range. What is important here is that the velocity range of this force, measured here in only one direction, is $\sim \pm 3.8\gamma/k$ corresponding to $\sim 7.6 v_c$, considerably larger than that for $F_{\rm rad}$.

Another possible reason for the large difference between the anticipated and measured forces is that the ARP conditions of equation (1) are not very well fulfilled for our laser parameters. For $\Omega = 60\gamma$ and $\delta_0 = 100\gamma$ the first condition of equation (1) is only weakly satisfied. Moreover, $\omega_s = 10\gamma$ gives $\dot{\delta} \sim 300\gamma^2$ so the condition $\dot{\delta} \gg 2\gamma\delta_0$ is also only weakly satisfied because $\dot{\delta}$ is only $1.5 \times 2\gamma\delta_0$. Nevertheless, the observed force significantly exceeds $F_{\rm rad}$.

For the data shown in figure 4, the laser frequency was symmetrically modulated around resonance, i.e. $\omega_\ell = \omega_a$, where ω_a is the atomic resonance frequency. Curiously, we observed larger forces when the laser was blue detuned from resonance and phases other than $\pi/4$ were used.

Figure 5 shows the deflection achieved when $\omega_\ell - \omega_a = 60\gamma$ and $\phi = \pi/10$. In this data, the distance from the interaction region to the detector was decreased from 70 to 30 cm so that atoms with larger transverse velocities would not bypass the MCP. The measured transverse velocity change in figure 5 is $\Delta v \sim 9\gamma/k \sim 175\hbar k/M$. For these data, 7 mm vertical slits were used to set the interaction time to 70τ and therefore the observed deflection corresponds to a force of $\sim 5 F_{\rm rad}$, closer to the ARP model force of $6.4 F_{\rm rad}$.

The unexpected result of forces considerably larger than $F_{\rm rad}$ under a wide range of relative phases ϕ and values of β has been predicted in numerical calculations [17]. A similar situation arises in the results of measurements of the bichromatic force, where laser parameters that satisfy the conditions of the π-pulse model result in a force that is much smaller than the maximum observed (see figure 1 of [12]).

5. Conclusions

We have demonstrated that the strength of the ARP force is $\gg F_{\rm rad}$ and its velocity range is $\gg v_c$, and thus it is comparable

in many ways to the bichromatic force. In some sense, the ARP force arises from a frequency modulation of light in counterpropagating beams whereas the bichromatic force arises from an amplitude modulation. Both can be described by appealing, simple models that involve the relative phase of the modulation of the counterpropagating beams. Yet the strongest force in both cases is observed under conditions that do not satisfy their respective models. These are interesting subjects for future study, both numerically and experimentally. Nevertheless, we believe that the fully implemented ARP force also has the capacity to stop our He* beam in a distance of less than 1 cm, much shorter than the 2 m required to stop He* with $F_{\rm rad}$.

Acknowledgments

This work was supported by the ONR and ARO.

References

[1] Metcalf H and van der Straten P 1999 *Laser Cooling and Trapping* (New York: Springer)
[2] Cohen-Tannoudji C and Phillips W 1990 *Phys. Today* Oct. **43** 33–40
[3] Dalibard J and Cohen-Tannoudji C 1985 *J. Opt. Soc. Am.* B **2** 1707
[4] Voitsekhovich V S *et al* 1988 *Sov. Phys.–Tech. Phys.* **33** 690
[5] Kazantsev A P and Krasnov I 1989 *J. Opt. Soc. Am.* B **6** 2140
See also Kazantsev A P and Krasnov I 1987 *Piz. Zh. Eksp. Teor. Fiz.* **46** 3333
[6] Voitsekhovich V S *et al* 1989 *JETP Lett.* **49** 161
Voitsekhovich V S 1991 *Sov. Phys.–JETP* **72** 219
[7] Grimm R *et al* 1990 *Phys. Rev. Lett.* **65** 1415
[8] Gupta R *et al* 1993 *Phys. Rev. Lett.* **71** 3087
[9] Grove T *et al* 1995 *Phys. Rev.* A **51** R4325
[10] Söding J *et al* 1997 *Phys. Rev. Lett.* **78** 1420 (Note that, in this work, $\gamma \equiv 1/2\tau$.)
[11] Williams M *et al* 1999 *Phys. Rev.* A **60** R1763
[12] Williams M *et al* 2000 *Phys. Rev.* A **61** 023408
[13] Cashen M and Metcalf H 2000 *Bull. Am. Phys. Soc.* **45** 58 C23 22
[14] Cashen M and Metcalf H 2001 *Phys. Rev.* A **63** 025406
[15] Cashen M *et al Phys. Rev.* A **64** at press
[16] Nebenzahl I and Szoke A 1974 *Appl. Phys. Lett.* **25** 327
[17] Voitsekovich V *et al* 1991 *Ukr. J. Phys.* **36** 192
[18] Demeter G *et al* 1998 *J. Opt. Soc. Am.* B **15** 16
[19] Allen L and Eberly L 1987 *Optical Resonance and Two-Level Atoms* (New York: Dover)
[20] Kawanaka J *et al* 1993 *Appl. Phys.* B **56** 21
[21] Mastwijk H *et al* 1998 *Eur. Phys. J.* D **4** 131
Mastwijk H 1997 *PhD Thesis* University at Utrecht